Available online at www.sciencedirect.com
ScienceDirect
Biosensors and Bioelectronics 22 (2007) 1776–1782
BIOSENSORS & BIOELECTRONICS
www.elsevier.com/locate/bios

Reagentless biosensor for hydrogen peroxide based on immobilization of protein in zirconia nanoparticles enhanced grafted collagen matrix

Shuizhen Zong [a,b], Yong Cao [c], Yuming Zhou [c], Huangxian Ju [a,*]

[a] *MOE Key Laboratory of Analytical Chemistry for Life Science, School of Chemistry and Chemical Engineering, Nanjing University, Nanjing 210093, PR China*
[b] *Department of Chemistry, Changshu Institute of Technology, Changshu 215500, PR China*
[c] *Department of Chemistry and Chemical Engineering, Southeast University, Nanjing 210096, PR China*

Received 13 April 2006; received in revised form 5 July 2006; accepted 23 August 2006
Available online 6 October 2006

Abstract

A novel matrix, zirconia nanoparticles enhanced grafted collagen (ZrO_2-grafted collagen) hybrid composite, for immobilization of protein and biosensing was developed. The scanning electron microscopy, UV–vis and Fourier transform infrared spectra, and electrochemical measurements showed that the matrix was well biocompatible and could retain the bioactivity of immobilized protein to a large extent. The direct electron transfer of the immobilized myoglobin (Mb) exhibited a couple of stable and well-defined redox peaks with the formal potential of −336 mV (versus SCE) in 0.1 M pH 7.0 PBS. This matrix could accelerate the electron transfer between Mb and the electrode with a surface-controlled process and an electron transfer rate constant of $3.58 \pm 0.35\ s^{-1}$ at 10–500 mV s^{-1}. The Mb immobilized in the matrix showed a high thermal stability up to 70 °C and an electrocatalytic activity to the reduction of hydrogen peroxide (H_2O_2) without the help of an electron mediator. The linear response range of the biosensor to H_2O_2 concentration was from 1.0 to 85.0 μM with the limit of detection of 0.63 μM at a signal-to-noise ratio of 3σ. The biosensor exhibited high sensitivity, acceptable stability and reproducibility. This work opened a way for the further study on the direct electron transfer and biosensing application of the immobilized protein in collagen-related matrices.

Keywords: Biosensor; Direct electron transfer; Grafted collagen; Zirconia nanoparticles; Myoglobin; Hydrogen peroxide

1. Introduction

The development of new biocompatible materials for the immobilization and biosensing applications of proteins has attracted considerable attention, since the direct contact of redox protein with uncoated electrode surface usually leads to significant changes in protein structure and function (Armstrongh et al., 1988; Lisdat et al., 1999; Xiao et al., 1999; Chattopadhyay and Mazumdar, 2000). Various matrices, such as colloidal gold nanoparticles (Xiao et al., 2000; Liu and Ju, 2002), SiO_2 nanoparticles (He et al., 2004; Kröning et al., 2004), zirconia nanoparticles (Liu et al., 2004a), titania nanoparticles (Zhang et al., 2004), hexagonal mesoporous silica (Dai et al., 2005) and porous titania sol–gel (Yu and Ju, 2002) have been developed for protein immobilization, some of them possess good biocompatibility and can accelerate the electron transfer of the immobilized proteins. A series of composites, such as sol–gel-derived tin oxide/gelatin composite films (Jia et al., 2005), carbon nanotubes and chitosan composite (Qian and Yang, 2006) have also been used for this purpose. The application of these composites leads to design of a series of reagentless amperometric biosensors.

Recently, advanced hybrid materials, especially nanoparticles enhanced hybrid materials, have been extensively synthesized. However, few researchers pay their attention to the biocompatibility and biosensing application of these materials. With the help of silica sol a porous gold nanoparticle–calcium carbonate hybrid material has been used for the assembly of horseradish peroxidase (HRP) on a glassy carbon electrode (Cai et al., 2006). The silica sol hinders the electron transfer between the immobilized HRP and electrode surface, though this process can be accelerated by the gold nanoparticles coexisting on elec-

* Corresponding author. Tel.: +86 25 83593593; fax: +86 25 83593593.
E-mail address: hxju@nju.edu.cn (H. Ju).

0956-5663/$ – see front matter © 2006 Elsevier B.V. All rights reserved.
doi:10.1016/j.bios.2006.08.032

trode surface. Thus, the formed biosensor shows low sensitivity for hydrogen peroxide (1.7 mA M^{-1} cm^{-2}) due to the presence of silica sol. In order to overcome this limitation it is necessary to develop a new method to fabricate nanoparticles enhanced hybrid materials for direct coimmobilization of hybrid material and redox protein and direct electron transfer of the immobilized protein. This work proposed a novel hybrid material, zirconia nanoparticles enhanced grafted collagen hybrid composite (ZrO_2-grafted collagen). The grafted collagen made it easier to form a stable membrane of hybrid material for immobilization of redox proteins. The immobilized protein showed excellent direct electrochemistry due to the presence of the nanoparticles.

Collagen is one of the biopolymers most extensively used to construct functionalized hybrid structures. To strengthen its mechanical and thermal stability extensive efforts have been made to mimic (Kinberger et al., 2002) or stabilize (Berisio et al., 2004) its soft conformation. Owing to the abundant oxygen and nitrogen atoms (Connolly et al., 1999) collagen molecule shows good affinity to metal oxide for stabilizing metal oxide nanoparticles away from their aggregation (Koide et al., 2002). By grafting collagen molecule with some lipophilic materials, such as methyl methacrylate (MMA) the noticeable improvement in biocompatibility of collagen has been obtained (Se and Aoyama, 2004). The hybrid material prepared in this work showed good biocompatibility, thermal and mechanical stability. The presence of nano-sized zirconia enhanced the tri-helix scaffold of collagen, increased the loading of myoglobin (Mb) and accelerated the electron transfer of immobilized Mb, which were significant for the preparation of a relatively sensitive reagentless biosensor for hydrogen peroxide (97 mA M^{-1} cm^{-2}). The prepared biosensor showed good analytical performance, indicating that the metal oxide nanoparticles-grafted collagen hybrid materials were suitable for protein immobilization and preparation of the third generation biosensors.

2. Experimental

2.1. Chemicals

Horse heart myoglobin (No. M-1882, type III) was purchased from Sigma and used as received. H_2O_2 (30%, w/v solution) was purchased from Shanghai Jinlu Chemical Engineering Ltd. Co (China). 2.0 mg ml^{-1} Mb solution was stored at a temperature of 4 °C as stock solution. ZrO_2 nanoparticles and grafted collagen were prepared according to the literatures (Lecomte et al., 1998; Cao et al., 2004), respectively. Zirconia enhanced grafted collagen tri-helix scaffold was prepared by dispersing ZrO_2 nanoparticles and grafting collagen in alcohol which was stirred overnight and refluxed at 60 °C for 8 h. The mixture was refrigerated for 2 h to remove impurities, and then separated in room temperature to obtain the hybrid composite (ZrO_2-grafted collagen powder). Other reagents were of analytical reagent grade. 0.1 M phosphate buffer solutions with different pH values were prepared by mixing the stock standard solutions of Na_2HPO_4 and NaH_2PO_4 and adjusting the pH with 0.1 M H_3PO_4 or NaOH. All solutions were made up with twice-distilled water.

2.2. Electrode preparation

The substrate graphite electrodes (geometric area: 26.4 mm^2) were polished before each experiment with 1.0, 0.3 and 0.05 μm α-alumina slurry (Beuhler), respectively, rinsed thoroughly with doubly distilled water between each polishing step, then sonicated in 1:1 nitric acid, acetone and doubly distilled water successively and allowed to dry at room temperature. ZrO_2-grafted collagen suspension was obtained by dispersing 4.0 mg ZrO_2-grafted collagen powder in 1.0 ml dimethyl sulfoxide (DMSO). After mixing 10 μl 2.0 mg ml^{-1} Mb solution with 5.0 μl ZrO_2-grafted collagen suspension, the mixture was cast on the graphite electrode to obtain Mb/ZrO_2-grafted collagen/DMSO/GE after slow evaporation of solvent and aged overnight in a sealed flask kept at a constant temperature of 18 °C. Alternatively, only 10 μl Mb or Mb/DMSO solution with the same Mb concentration and 5.0 μl ZrO_2-grafted collagen suspension were cast on the electrodes to form Mb/GE, Mb/DMSO/GE or ZrO_2-grafted collagen/DMSO/GE modified electrode, respectively. Prior to electrochemical experiments, the modified electrodes were rinsed thoroughly with doubly distilled water and kept in 0.1 M pH 7.0 PBS at 4 °C.

2.3. Measurements

Electrochemical measurements were performed on a CHI 730A electrochemical analyzer (CHI Co., China) at 18 ± 2 °C with a conventional three-electrode system with the modified graphite electrode (GE) as working electrode, a platinum wire as auxiliary electrode and a saturated calomel electrode (SCE) as reference against which all potentials were measured. The thermal stability of the Mb/ZrO_2-grafted collagen/DMSO/GE was examined by increasing the cell temperature and keeping the corresponding temperature for 20 min to record the cyclic voltammograms. The amperometric measurements were performed in a stirred cell at 18 ± 2 °C by applying a potential of −350 mV with successive additions of H_2O_2 solution to the buffer solution. The sensor response was measured as the difference between total and residual currents. All experimental solutions were deoxygenated by bubbling highly pure nitrogen for 15 min and maintained under nitrogen atmosphere during measurements.

UV–vis absorbance spectroscopy was performed using a UV–vis-3100-Nir Recording Spectrophotometer (Shimadzu, Japan). Fourier transform infrared (FT-IR) spectra were recorded on a Vector 22 FT-IR spectrometer (Bruker). For morphological analysis, the sample films were prepared in the same way as that for voltammetric measurements on different slides cleaned with nitric acid and the mixture of H_2SO_4:H_2O_2 (1:1, v/v). After coated with Au film to improve the conductivity, these films were examined under a scanning electron microscope (SEM, LEO 1530 VP, Germany) at 5.00 kV.

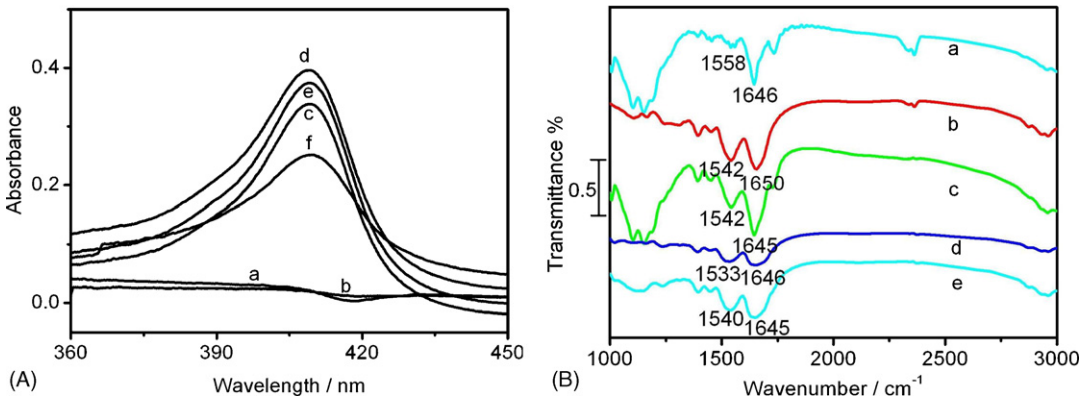

Fig. 1. (A) UV–vis spectra of DMSO (a), ZrO_2-grafted collagen/DMSO (b), Mb (c), Mb/ZrO_2-grafted collagen (d), Mb/ZrO_2-grafted collagen/DMSO (e) and Mb/DMSO (f) solutions. (B) FT-IR spectra of ZrO_2-grafted collagen (a), Mb (b), Mb/ZrO_2-grafted collagen (c), Mb/DMSO (d) and Mb/ZrO_2-grafted collagen/DMSO (e) films.

3. Results and discussion

3.1. UV–vis and FT-IR analyses

Fig. 1A shows the UV–vis spectra of different systems. No adsorption of DMSO and ZrO_2-grafted collagen/DMSO is observed (curves a and b). All suspensions or solutions containing Mb display a maximum adsorption at 409 nm (curves c–f). Obviously, the adsorption peak is attributed to the Soret band of Mb, which usually occurs at 409 nm at a neutral pH (Ray et al., 2005). No shift of the Soret band upon mixing of Mb with ZrO_2-grafted collagen or DMSO was observable. Thus, the interaction between ZrO_2-grafted collagen and Mb molecules did not change the fundamental microenvironment of Mb. The Mb mixed in these systems retained its natural secondary structure.

The FT-IR spectra of Mb, Mb/ZrO_2-grafted collagen, Mb/DMSO and Mb/ZrO_2-grafted collagen/DMSO films (Fig. 1B) showed the interaction between ZrO_2-grafted collagen and Mb. The FT-IR spectrum of ZrO_2-grafted collagen showed the amide I and amide II infrared absorbance of collagen at 1646 and 1558 cm^{-1} (curve a). The absorption bands for the amide I and amide II in the Mb/ZrO_2-grafted collagen/DMSO and Mb/ZrO_2-grafted collagen film were located at 1645, 1540, 1645 and 1542 cm^{-1} (curves e and c), respectively, which were nearly the same as 1650 and 1542 cm^{-1} obtained for the protein itself (curve b). The presence of DMSO resulted in great decrease of the absorption (curve d) and greater shift in the peak position of amide II infrared absorbance than those in presence of the hybrid composite. Previous studies demonstrated that the absorption band would diminish upon the full protein denaturation (Nassar et al., 1995). In comparison with the amide I and amide II adsorption bands in presence of only DMSO (curve d), the hybrid composite increased the adsorption (curve e), thus improving greatly the microenvironment for retaining the natural structure of the immobilized Mb. The small shift in the two absorption peaks suggested the interaction between ZrO_2-grafted collagen and Mb.

3.2. SEM characterization

Fig. 2 shows the SEM images of three membranes. The micrograph of ZrO_2-grafted collagen film displayed a chemically clean uniform three-dimensional porous structure. This three-dimensional structure possessed a very narrow particle size distribution with the average diameter ranged between 30 and 40 nm (Fig. 2a). Dispersing of Mb onto the glass slice, the Mb molecules aggregated together in the absence of DMSO or ZrO_2-grafted collagen (Fig. 2b). After mixing of Mb with ZrO_2-grafted collagen/DMSO, a well-distributed layer of the film could be formed (Fig. 2c). In this case, the ZrO_2-grafted collagen hybrid composites were surrounded by Mb molecules, leading to bigger size of nanoparticles. The uniform porous structure increased the homogeneous loading of

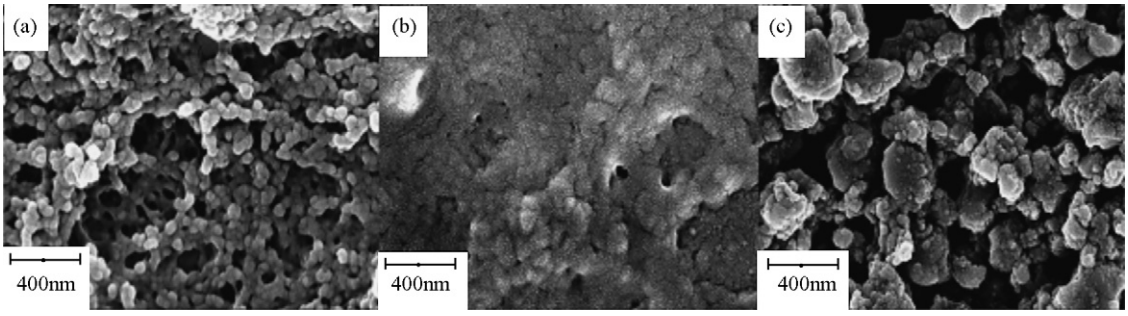

Fig. 2. Scanning electron micrographs of ZrO_2-grafted collagen (a), Mb (b) and Mb/ZrO_2-grafted collagen (c) on a glass slice.

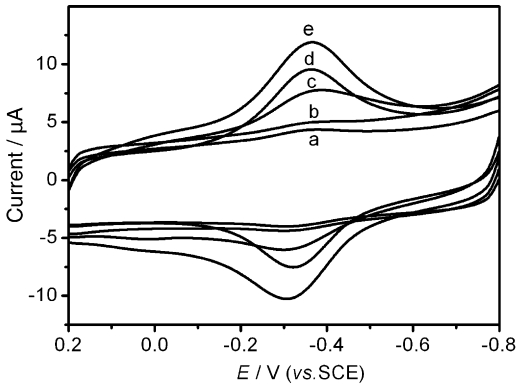

Fig. 3. Cyclic voltammograms of ZrO_2-grafted collagen/DMSO/GE (a), GE (b), Mb/GE (c), Mb/DMSO/GE (d) and Mb/ZrO_2-grafted collagen/DMSO/GE (e) in 0.1 M pH 7.0 PBS at 50 mV s^{-1}.

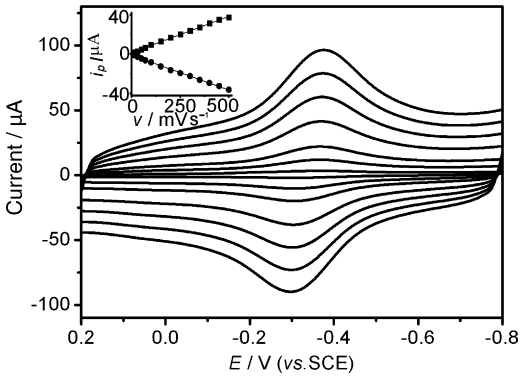

Fig. 4. Cyclic voltammograms of Mb/ZrO_2-grafted collagen/DMSO/GE in 0.1 M pH 7.0 PBS at 10, 50, 100, 200, 300, 400 and 500 mV s^{-1} (from lowest to highest current). *Inset*: Plot of peak current vs. scan rate.

enzyme molecules, provided a good preparation reproducibility of the immobilized Mb electrodes and prevented the leaking of enzyme.

3.3. Direct electrochemistry of Mb/ZrO_2-grafted collagen/DMSO modified electrode

The cyclic voltammogram of Mb/ZrO_2-grafted collagen/DMSO/GE displayed a couple of stable and well-defined redox peaks at −308 and −363 mV at 50 mV s^{-1} (curve e in Fig. 3). No obvious electrochemical response was observed at both ZrO_2-grafted collagen/DMSO/GE and GE (curves a and b in Fig. 3), though the former displayed a lower background. Thus, these peaks were attributed to the redox reaction of the electroactive center of Mb. Although the Mb/GE and the Mb/DMSO/GE could also display a couple of redox peaks of Mb (curves c and d in Fig. 3), these peak currents were much smaller than those at the Mb/ZrO_2-grafted collagen/DMSO/GE. The improvement in direct electrochemistry in presence of DMSO alone was due to the decrease of the dielectric constant of the microenvironment around Mb molecules, which decreased the reorganization energy of biological electron transfer (Zhou, 1994). The further increase of the peak currents indicated ZrO_2-grafted collagen was very important for facilitating the electron exchange. From the integration of the reduction peak of Mb/ZrO_2-grafted collagen/DMSO/GE at different scan rates, an average surface coverage (Γ^*) of Mb was calculated to be $7.24 \pm 0.23 \times 10^{-10}$ mol cm^{-2}, which was much larger than 5.18×10^{-11} mol cm^{-2} at Mb-agarose hydrogel electrode (Liu et al., 2004b), 8.85×10^{-11} mol cm^{-2} at $\{[SiO_2\text{-}(Mb/PSS)_m]/PEI\}_n$ (Liu et al., 2004c), indicating a better loading of the Mb in the hybrid composite matrix.

The formal potential $E_{1/2}$ of the heme $Fe^{III/II}$ couple in Mb/ZrO_2-grafted collagen/DMSO/GE, estimated as the midpoint of reduction and oxidation potentials, was -336 ± 3 mV in 0.1 M pH 7.0 PBS. This value was similar to those of −323 mV at Mb-DHP-PDDA (Wang and Hu, 2001), −362 mV at Mb-AQ (Hu and Rusling, 1997), −342 mV at Mb-silk fibroin (Wu et al., 2006) and −342 mV at Mb-colloidal gold (Liu and Ju, 2003), suggesting that most molecules preserved their native structure after being entrapped in the ZrO_2-grafted collagen matrix. The cyclic voltammogram of the Mb/ZrO_2-grafted collagen/DMSO/GE showed a nearly equal height of reduction and oxidation peaks at the same scan rate (Fig. 4). With an increasing scan rate from 10 to 500 mV s^{-1}, the anodic and cathodic peak potentials of the Mb showed small shift and the redox peak currents increased linearly (inset in Fig. 4), indicating a surface-controlled electrode process. The peak-to-peak separations of the cyclic voltammograms at 50, 70, 100, 150, 200, 250, 300, 350, 400, 450 and 500 mV s^{-1} were 65, 71, 78, 75, 79, 79, 78, 79, 82, 83 and 85 mV, respectively. Considering the α value between 0.3 and 0.7 and the peak-to-peak separation less than 100 mV, the electron transfer rate constant k_s was estimated according to the formula $k_s = mnFv/RT$ (Laviron, 1979) to be 3.58 ± 0.03 s^{-1}, where m is a parameter related to the peak-to-peak separation. The k_s value was larger than those of 0.93 s^{-1} for Mb immobilized on DL-homocysteine self-assembled gold electrode (Zhang and Li, 2001), 1.34 s^{-1} for Mb immobilized in silk fibroin film (Wu et al., 2006), 1.2 s^{-1} for Mb entrapped in agarose hydrogel film in room-temperature ionic liquid (Wang et al., 2005), suggesting a reasonably fast electron transfer between the immobilized Mb and the electrode due to the presence of ZrO_2-grafted collagen.

3.4. Effect of solution pH on the direct electron transfer of immobilized Mb

Fig. 5 shows the effect of solution pH on the direct electrochemistry of the immobilized Mb. With the increasing of solution pH from 4.0 to 10.0 the negative shift of both reduction and oxidation peak potentials was observed. In general, all changes in the peak potentials and currents with solution pH were reversible in the pH range from 4.0 to 10.0, that was, the same cyclic voltammograms could be obtained if the electrode was transferred from a solution with a different pH value to its original solution. The plot of formal potential versus pH showed a slope of −43.9 mV pH^{-1} ($R = 0.9997$) (inset in Fig. 5), which was close to −48.7 mV pH^{-1} for Mb-clay films (Zhou et al., 2002) and the expected value of −57.8 mV pH^{-1} at 291 K,

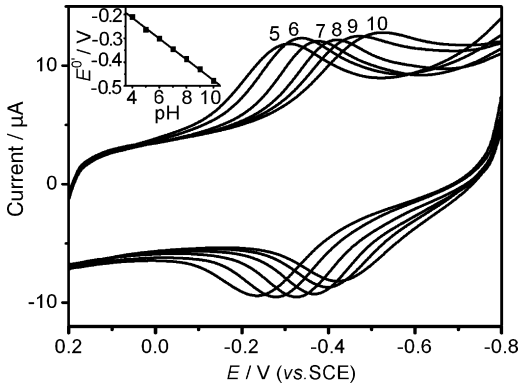

Fig. 5. Cyclic voltammograms of Mb/ZrO_2-grafted collagen/DMSO/GE in PBS with various pH values at 50 mV s^{-1}. *Inset*: Plot of formal potential vs. pH.

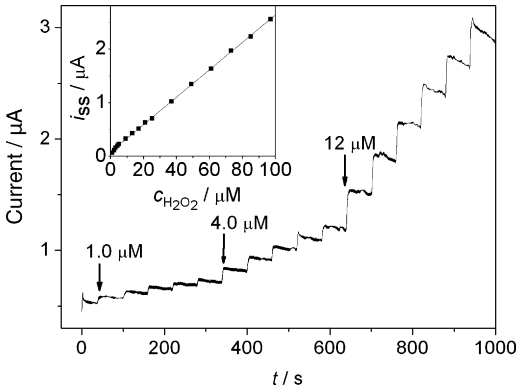

Fig. 6. Amperometric response of the sensor at −350 mV upon succcessive additions of 1.0, 4.0 and 12.0 μM H_2O_2 pH 7.0 PBS. *Inset*: Plot of steady-state current vs. H_2O_2 concentration.

indicating that one proton participated in the electron transfer process (Chen et al., 1999; Sun et al., 2000).

3.5. Thermal stability of Mb/ZrO_2-grafted collagen/DMSO/GE

Thermal stability is a measure of the ability of the biosensor to withstand elevation in temperature. In 0.1 M pH 7.0 PBS the cathodic peak current of the Mb/ZrO_2-grafted collagen/DMSO/GE increased with an increasing temperature from 20 to 70 °C. If the temperature was over 80 °C, some milk-white globules appeared on the electrode surface because of the protein denaturation, meanwhile, the cathodic peak current of the Mb/GE began to decrease. In absence of ZrO_2-grafted collagen the decrease of peak current occurred when the temperature was up to 51 °C. The good biocompatibility in the presence of ZrO_2-grafted collagen led to an improvement of the thermal stability.

3.6. Electrocatalysis of Mb/ZrO_2-grafted collagen/DMSO/GE to reduction of H_2O_2

Upon addition of H_2O_2 to 0.1 M pH 7.0 PBS, the shape of cyclic voltammogram for the direct electron transfer of immobilized Mb changed dramatically with an increase of reduction peak current and a decrease of oxidation peak current, while the change of cyclic voltammogram of bare or ZrO_2-grafted collagen/DMSO modified GE was very small, displaying an obvious electrocatalytic behavior of the Mb to the reduction of H_2O_2. Fig. 6 shows the amperometric response of the Mb/ZrO_2-grafted collagen/DMSO/GE at an applied potential of −350 mV on successive additions of H_2O_2 to a stirring 0.1 M pH 7.0 PBS. Upon addition of an aliquot of H_2O_2 to the buffer solution, the reduction current increased steeply to reach a stable value. The modified electrode achieved 95% of the maximum steady-state-current in less than 9 s. This demonstrated clearly that the electrocatalytic response was very fast. Although the current steps for the catalyzed signal displayed a decreasing current over time, we did not observe the difference among the signals determined for several times at the same concentration after H_2O_2 was added for 25 s. The catalytic current was stable and reproducible after 25 s. The decrease was due to the uneven concentration of H_2O_2 on the electrode surface that resulted from the addition of new H_2O_2 solution.

The linear response range of the sensor to H_2O_2 concentration was from 1.0 to 85.0 μM with a linear regression equation of I (μA) = 0.084 + 0.026c (μM) (R = 0.9998, n = 16). From the slope of 0.026 μA μM^{-1}, the limit of detection was estimated to be 0.63 μM at a signal-to-noise ratio of 3σ. The relative standard deviation for five successive measurements of 50.0 μM hydrogen peroxide was less than 3.6%. The limit of detection was lower than those of 8.0 μM for Mb immobilized in hydroxyethylcellulose (Liu et al., 2006) and 4.0 μM for Mb in ZrO_2/chitosan (Zhao et al., 2005). Based on the fast direct electron transfer and electrocatalytic behavior of the immobilized Mb to the reduction of H_2O_2, the Mb/ZrO_2-grafted collagen/DMSO/GE showed a sensitivity of 97 mA M^{-1} cm^2, which was much higher than those of 36 mA M^{-1} cm^{-2} for Mb in pluronic film (Shan et al., 2005) and 1.7 mA M^{-1} cm^{-2} for HRP in porous gold nanoparticle-$CaCO_3$ hybrid material immobilized with silica sol–gel (Cai et al., 2006).

The enzymatic saturation response was observed when the concentration of H_2O_2 was higher than 85 μM, showing a characteristic of the Michaelis–Menten kinetic mechanism. The apparent Michaelis–Menten constant (K_M^{app}), a reflection of both the enzymatic affinity and the ratio of microscopic kinetic constants dependent on the microstructure and microenvironment of the whole sensor surface, was obtained to be 0.025 ± 0.005 mM from the electrochemical version of the Linweaver–Burk equation (Kamin and Wilson, 1980). The K_M^{app} value was much smaller than those of 1.3 mM for Mb immobilized on silver nanoparticles (Gan et al., 2004), 1.53 mM for Mb/ZrO_2/chitosan (Zhao et al., 2005) and 0.65 mM for Mb immobilized on colloidal gold nanoparticles (Liu and Ju, 2003). Thus, the good biocompatibility and porous structure increased the affinity of the immobilized Mb for H_2O_2.

3.7. Interference study

Possible interference that might occur in real samples was tested. No significant interference could be observed for mat-

ters, such as SO_4^{2-}, CO_3^{2-}, ClO_3^-, Cl^-, Br^-, I^-, glycin and ascorbic acid, at concentrations 10 times that of hydrogen peroxide at 50.0 μM, indicating these matters coexisting in the sample matrix did not affect the determination of hydrogen peroxide. These results indicated this method was reliable. However, Fe^{3+} might be a main interference to Mb for the electrocatalytic reduction of hydrogen peroxide. When the concentration of Fe^{3+} was increased to five times that of hydrogen peroxide, the peak current changed approximately 6.4%. This possibly resulted from the interaction between Fe^{3+} and hydrogen peroxide similar to that reported previously (Wang et al., 2002) and could be excluded by adding EDTA in the sample solution.

With the purpose to demonstrate the applicability of the proposed biosensor for real sample analysis, 35 and 70 μM hydrogen peroxide solution were added into rain water samples, respectively. The average recovery of the biosensor was 99.2% ($n = 5$) and 105.0% ($n = 5$), respectively. The rain water sample without adding H_2O_2 did not show any detectable signal.

3.8. Stability and reproducibility of the H_2O_2 biosensor

When it was cyclically swept between −0.8 and +0.2 V in 0.1 M pH 7.0 PBS at 50 mV s^{-1} for 40 times, the peak current measurements corresponding to the direct electrochemistry of the immobilized Mb gave a relative standard deviation of 1.45%. This sensor could retain 93.0% of its initial current response after 50-day storage in 0.1 M pH 7.0 PBS at 4 °C, showing better stability than Mb immobilized in hydroxyethylcellulose (Liu et al., 2006) and Mb in ZrO_2/chitosan (Zhao et al., 2005). It was obvious that the presence of ZrO_2-grafted collagen enhanced the stability of the biosensor. The relative standard deviation for six successive determinations at a H_2O_2 concentration of 60 μM was 3.18 %. The fabrication of five electrodes, made independently, showed a good reproducibility with a relative standard deviation of 5.47% for the current determination of 60.0 μM H_2O_2.

4. Conclusions

This work demonstrated that the proposed ZrO_2-grafted collagen hybrid composite was highly useful for bioelectrochemical and biosensing applications. This material possessed excellent biocompatibility and thermal stability. The cyclic voltammogram of Mb/ZrO_2-grafted collagen/DMSO modified electrode exhibited a pair of redox peaks corresponding to the electroactive center of Mb with a single proton transfer. ZrO_2-grafted collagen retained the activity of the immobilized Mb and facilitated the direct electron exchange between Mb and electrode. The H_2O_2 biosensor based on the fast direct electron transfer of the Mb immobilized in ZrO_2-grafted collagen matrix exhibited wide linear detection range, acceptable reproducibility, operational convenience and storage stability. The immobilized Mb displayed a high affinity to H_2O_2. The novel ZrO_2-grafted collagen hybrid composite provided a good matrix for the further study on the direct electron transfer of proteins and development of biosensors.

Acknowledgements

This work was supported by the National Science Fund for Distinguished Young Scholars (20325518) and Creative Research Groups (20521503) and the Key Program from the National Natural Science Foundation of China (20535010).

References

Armstrongh, F., Hill, A., Walton, N., 1988. Acc. Chem. Res. 21, 407–413.
Berisio, R., Granata, V., Vitagliano, L., Zagari, A., 2004. J. Am. Chem. Soc. 126, 11402–11403.
Cai, W.Y., Xu, Q., Zhao, X.N., Zhu, J.J., Chen, H.Y., 2006. Chem. Mater. 18, 279–284.
Cao, Y., Zhou, Y.M., Shan, Y., Ju, H.X., Xue, X.J., Wu, Z.H., 2004. Adv. Mater. 16, 1189–1192.
Chattopadhyay, K., Mazumdar, S., 2000. Bioelectrochem. Bioenerg. 53, 17–24.
Chen, X.L., Hu, N.F., Zeng, Y.H., Rusling, J.F., Yang, J., 1999. Langmuir 15, 7022–7030.
Connolly, S., Rao, S.N., Rizza, R., Zaccheroni, N., Fitzmaurice, D., 1999. Coord. Chem. Rev. 185/6, 277–295.
Dai, Z.H., Ju, H.X., Chen, H.Y., 2005. Electroanalysis 17, 862–868.
Gan, X., Liu, T., Zhong, J., Liu, X.J., Li, G.X., 2004. ChemBioChem 5, 1686–1691.
He, P.L., Hu, N.F., Rusling, J.F., 2004. Langmuir 20, 722–729.
Hu, N.F., Rusling, J.F., 1997. Langmuir 13, 4119–4125.
Jia, N.Q., Zhou, Q., Liu, L., Yan, M.M., Jiang, Z.Y., 2005. J. Electroanal. Chem. 580, 213–221.
Kamin, R.A., Wilson, G.S., 1980. Anal. Chem. 52, 1198–1205.
Kinberger, G.A., Cai, W., Goodman, M., 2002. J. Am. Chem. Soc. 124, 15162–15163.
Koide, T., Yuguchi, M., Kawakita, M., Konno, H., 2002. J. Am. Chem. Soc. 124, 9388–9389.
Kröning, S., Scheller, F.W., Wollenberger, U., Lisdat, F., 2004. Electroanalysis 6, 253–259.
Laviron, E., 1979. J. Electroanal. Chem. 101, 19–28.
Lecomte, A., Blanchard, F., Dauger, A., Silva, M.C., Guinebretière, R., 1998. J. Non-Cryst. Solids 225, 120–124.
Lisdat, F., Ge, B., Scheller, F.W., 1999. Electrochem. Commun. 1, 65–68.
Liu, S.Q., Dai, Z.H., Chen, H.Y., Ju, H.X., 2004a. Biosens. Bioelectron. 19, 963–969.
Liu, S.Q., Ju, H.X., 2002. Anal. Biochem. 307, 110–116.
Liu, S.Q., Ju, H.X., 2003. Electroanalysis 15, 1488–1493.
Liu, H.H., Tian, Z.Q., Lu, Z.X., Zhang, Z.L., Zhang, M., Pang, D.W., 2004b. Biosens. Bioelectron. 20, 294–304.
Liu, H.Y., Rusling, J.F., Hu, N.F., 2004c. Langmuir 20, 10700–10705.
Liu, X.J., Chen, T., Liu, L.F., Li, G.X., 2006. Sensors and Actuators B 113, 106–111.
Nassar, A.-E.F., Willis, W.S., Rusling, J.F., 1995. Anal. Chem. 67, 2386–2392.
Qian, L., Yang, X.R., 2006. Talanta 68, 721–727.
Ray, A., Feng, M.L., Tachikawa, H., 2005. Langmuir 21, 7456–7460.
Se, K., Aoyama, K., 2004. Polymer 45, 79–85.
Shan, W.J., He, P.L., Hu, N.F., 2005. Electrochim. Acta 51, 432–440.
Sun, H., Hu, N.F., Ma, H.Y., 2000. Electroanalysis 12, 1064–1070.
Wang, H.Y., Guan, R., Fan, C.H., Zhu, D.X., Li, G.X., 2002. Sens. Actuators B 84, 214–218.
Wang, L.W., Hu, N.F., 2001. J. Colloid Interface Sci. 236, 166–172.
Wang, S.F., Chen, T., Zhang, Z.L., Shen, X.C., Lu, Z.X., Pang, D.W., Wong, K.Y., 2005. Langmuir 21, 9260–9266.
Wu, Y.H., Shen, Q.C., Hu, S.S., 2006. Anal. Chim. Acta 558, 179–186.
Xiao, Y., Ju, H.X., Chen, H.Y., 2000. Anal. Biochem. 278, 22–28.

Xiao, Z.G., Lavery, M.J., Bond, A.M., Wedd, A.G., 1999. Electrochem. Commun. 1, 309–314.
Yu, J.H., Ju, H.X., 2002. Anal. Chem. 74, 3579–3583.
Zhang, H.M., Li, N.Q., 2001. Bioelectrochem. 53, 97–101.
Zhang, Y., He, P.L., Hu, N.F., 2004. Electrochim. Acta 49, 1981–1988.
Zhao, G., Feng, J.J., Xu, J.J., Chen, H.Y., 2005. Electrochem. Commun. 7, 724–729.
Zhou, H.X., 1994. J. Am. Chem. Soc. 116, 10362–10375.
Zhou, Y.L., Hu, N.F., Zeng, Y.H., Rusling, J.F., 2002. Langmuir 18, 211–219.